J Mol Model (2015) 21: 31
DOI 10.1007/s00894-015-2575-7

ORIGINAL PAPER

Study on wrinkling in graphene under gradient shear by molecular dynamics simulation

Jianzhang Huang · Qiang Han

Received: 9 October 2014 / Accepted: 4 January 2015 / Published online: 31 January 2015

Abstract The formation and development mechanisms of wrinkles in a rectangular single layer graphene sheet (SLGS) subjected to in-plane gradient shear displacements are investigated through molecular dynamics (MD) simulations. The growth and propagation process of the SLGS wrinkling is elucidated by the developing atomic out-of-plane displacements of the key atoms. It reveals that the shape of SLGS and loading condition have a significant effect on the SLGS wrinkling deformation. The dependences of the wrinkling amplitude, wavelength, and out-of-plane displacements on the applied gradient shear displacements are obtained with MD simulations. The effects of aspect ratio, temperature, and loading grads on wrinkling in graphene are also studied.

Keywords Gradient shear · Graphene · Molecular dynamics · Wrinkle

Introduction

Graphene sheet, a current focus of nanomechanics research, has drawn significant attention owing to its remarkable mechanical, thermal, and electrical properties. Graphene has become an ideal candidate for nano-devices, i.e., nano-sensors, nano-resonators, and nano-transistors due to its excellent physical properties [1]. Wrinkling is a common phenomenon in two-dimensional (2D) structure, i.e., film and membranes. Graphene, a real 2D material with one-atom-thickness, is easy to wrinkle as a result of its relatively small bending rigidity. The wrinkles in graphene were first discovered by Meyer et al. in 2007 [2]. Graphene wrinkling may be triggered by several external loads, such as the chemical functional group effect, thermal fluctuation, mechanical strain, and structural defect of substrate [3, 4]. The extraordinary mechanical, electrical, thermal, and chemical properties of graphene can be significantly influenced by the wrinkling [5–7]. Zhu et al. [8] reported that the wrinkling in graphene could degrade the on-off ratio and contribute a significant resistance to the overall device, from an application standpoint. Chen et al. [9] demonstrated that the wrinkling decreased the thermal conductivity value of graphene based on the results obtained by micro-Raman mapping. Graphene have been considered as potential material for transparent conductive film, and the high density wrinkles make graphene an ideal candidate for application in hydrogen storage, supercapacitors, and nanomechanical devices [10]. The wrinkles also increase the graphene reinforcement effect in composites by enhancing the adhesion and interlock bonding between graphene and polymers [11, 12]. A high pseudo-magnetic field introduced by the graphene wrinkling was discovered by Levy et al. [13]. Meanwhile, the wrinkling configurations, amplitude, and wavelength can be controlled to meet the needs of graphene engineering applications. Thus, investigating and understanding the mechanisms of graphene wrinkling not only have significant academic value, but also the engineering potential application.

Up to now, the graphene wrinkling research works have been focused on the effects of wrinkling on the physical properties of graphene, more than elucidating the physical nature of the wrinkling mechanism. The graphene wrinkling simulations research works in public literature are concerned with the wrinkling in graphene with different structural shapes subjected to simple tension, compression or shear and clamped

J. Huang · Q. Han (✉)
School of Civil Engineering and Transportation,
South China University of Technology, Guangzhou,
Guangdong, People's Republic of China
e-mail: emqhan@scut.edu.cn
URL: http://www.scut.edu.cn

J. Huang
e-mail: h.jianzhang@mail.scut.edu.cn

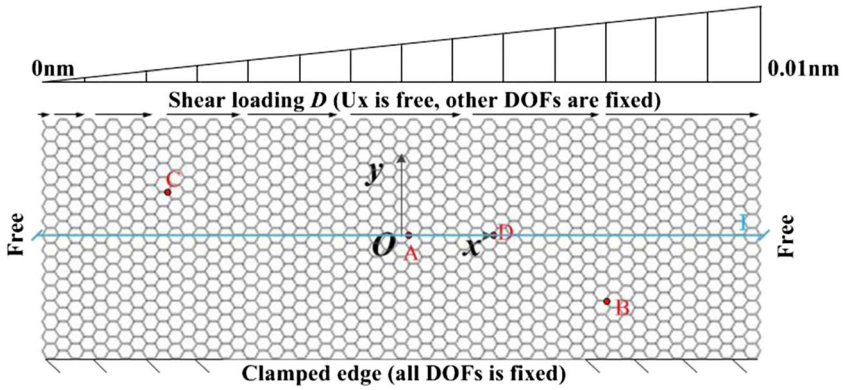

Fig. 1 The model of SLGS

boundary condition [4, 14–19]. These studies concentrated on the wrinkling configuration, wavelength, and amplitude. Few efforts have been devoted to studies on the effects of gradient shear loading on graphene wrinkling. In this paper, the wrinkling mechanism zigzag rectangluar SLGS subjected to gradient shear are investigated based on molecular dynamics (MD) simulations. The evolution mechanism of wrinkling is elucidated by the atomic out-of-plane displacement development of the key atoms and wrinkling parameters. The dependencies of wrinkling parameters on applied shear displacements are obtained. The effects of temperature, aspect ratio, and loading grads on graphene wrinkling are investigated at the end.

Methods

Molecular dynamics simulation

A zigzag rectangular SLGS (12.053×4.052 nm^2) subjected to in-plane gradient shear and given boundary conditions are shown in Fig. 1. The upper edge of graphene is the load boundary, of which degrees of freedom (DOF) in y and z dimension are fixed while the DOF in x dimension is free. The bottom edge of graphene is the clamped boundary in which all degrees of freedom are fixed. The left and right edges of graphene are free boundaries. Four key points A(0.1418 nm, 0.0614 nm), B(3.4741 nm, −1.0438 nm), C(−3.9704 nm, 0.7982 nm), D(1.5598 nm, 0.0614 nm), and section line I (y=0.0614 nm) on the graphene surface are also shown in Fig. 1. The key points are distributed across the graphene, located in the possible wrinkling region and their variations of out-of-plane displacement are used to reflect the wrinkling evolution and propagation.

The LAMMPS MD code is utilized. All the MD simulations are performed under NVT ensemble using the adaptive intermolecular reactive empirical bond-order (AIREBO) potential function [20] for molecular interaction and velocity-Verlet algorithm for integration with a time step of 1 fs. The non-periodical boundaries are set for the global simulation box in each dimension. The temperature is maintained at 0.01 K and relaxed every 0.1 ps using Nose-Hoover

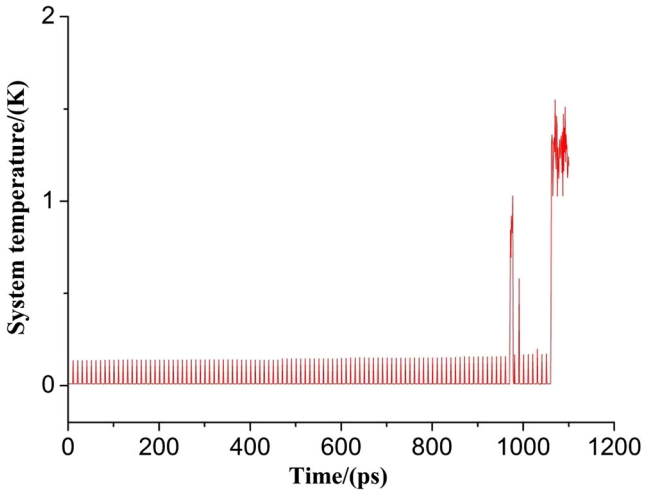

Fig. 2 Variation of the system temperature during simulation

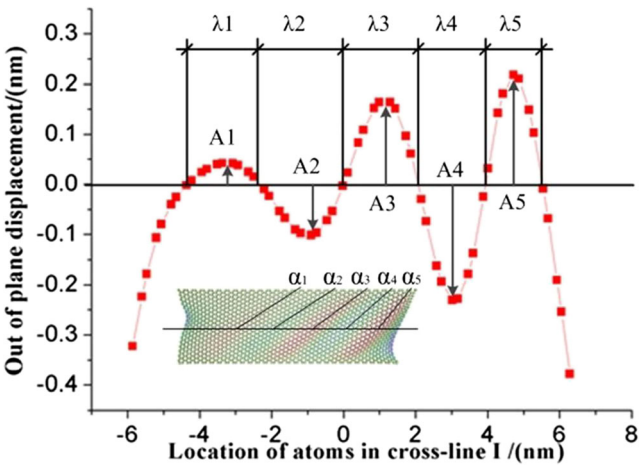

Fig. 3 Section line I. (d_{max}=0.86 nm)

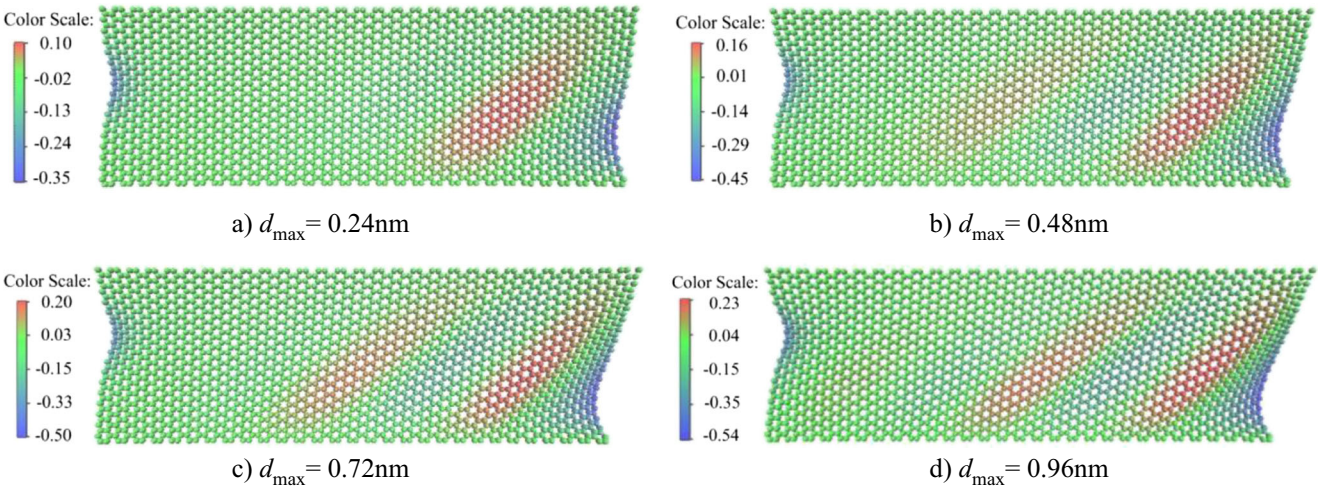

Fig. 4 Wrinkling configurations (unit: nm) **a** d_{max}=0.24 nm **b** d_{max}=0.48 nm **c** d_{max}=0.72 nm **d** d_{max}=0.96 nm

thermostat. The value of drag term is set as 0.2. After the energy minimization process, the gradient shear displacements, D which linearly changes from 0 to 0.01 nm (loading grads k_d is 8.333×10^{-4}), are applied. The "*ramp*" style of "displace_atoms" command is used to simulate the load. The atoms on the bottom edge are fixed and the atoms on the upper edge are displaced with an amount between 0 and 0.01 nm in x-dimension depending on their coordinate in x-dimension. The loading displacements are applied at every 10, 000 steps and repeat 110 times. The C-C bond length is 0.1418 nm with a 0.2 nm cutoff distance.

The variation of the system temperature with time is shown as Fig. 2. The system temperature is well controlled during the first 970 ps of the simulation. After 970 ps, there is a sudden rise of temperature due to the energy released by wrinkling evolution going into the mature stage. Then the temperature goes back to the normal level instantly. At about 1060 ps, the system temperature increases abruptly and goes beyond control, owing to the energy released by the breakage of the C-C bonds on graphene. Therefore, in this paper, the graphene wrinkling parameters and configurations are investigated based on the results obtained from the first 970 ps of the simulation. The wrinkling evolution is also studied not involving the breakage of graphene.

The simulations of different size of graphene wrinkling are carried out. Aspect ratio is defined as the ratio of length to width of rectangular SLGS. The width of graphene is set as 4.052 nm. The aspect ratio ranges from 1 to 7 by changing the graphene's length. The temperature is 0.01 K and loading grads k_d is 8.333×10^{-4}.

For temperature effect simulations, the size of rectangular SLGS is 12.053×4.052 nm^2 (aspect ratio is 3) and the loading grads k^d is 8.333×10^{-4}. The temperatures are set as different value ranging from 0.01 to 500 K.

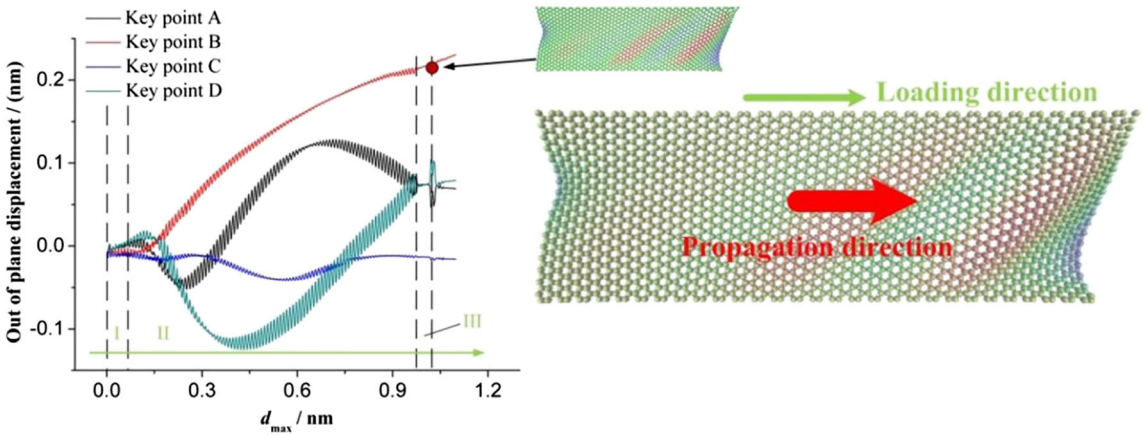

Fig. 5 Atomic displacements of key points and wrinkling propagation

Table 1 Wrinkling parameters

d_{max} (nm)	$\overline{\eta}_A$ (nm)	$\overline{\eta}_\lambda$ (nm)	$\overline{\eta_A/\eta_\lambda}$	n	$\overline{\eta}_\alpha$ (°)	w_E (nm)
0.24	0.08	3.80	0.024	2(1, 1)	37.353	0.35
0.48	0.13	2.56	0.054	3(2, 1)	39.321	0.45
0.72	0.14	2.30	0.070	4(2, 2)	40.183	0.50
0.96	0.15	1.96	0.080	5(3, 2)	40.656	0.54

For loading grads effect simulations, the size of rectangular SLGS is 12.053×4.052 nm^2 (aspect ratio is 3) and the temperature is 0.01 K. The different loading grads k_d are set as 5.000×10^{-4}, 6.667×10^{-4}, 8.333×10^{-4}, 1.000×10^{-3}, 1.167×10^{-3}, and 1.333×10^{-3} respectively.

Wrinkling parameter

Graphene wrinkling triggered by the external loads is formed on the graphene surface with a distinct direction and self-similarity. The wrinkling number n is defined as the total number of wrinkling crest and trough, e.g., n=5(3, 2) means the wrinkling number is five, including three wrinkling crests and two troughs.

For the wrinkling characteristic description, the global wrinkling parameters $\overline{\eta}$ which reflect the mean level of the graphene wrinkling characteristics are defined by the expression:

$$\overline{\eta} = \frac{1}{n}\sum_{i=1}^{n}\eta_i.$$

The η represents a given wrinkling parameter, i.e., wrinkling wavelength η_λ, amplitude η_A, angle η_α, and the ratio of wrinkling amplitude to wavelength η_A/η_λ. The d_{max} is the displacement of the rightmost atom of the graphene's upper edge. The wrinkling parameters are shown in Fig. 3, and the direction angle η_α means the angle between wrinkling direction and horizontal direction. The morphology of the wrinkle could be reflected by the η_A/η_λ. The w_E represents the maximum of the out-of-plane displacements of the graphene. The parameter $n\overline{\eta}_\lambda/L$ reflects the extent of graphene wrinkles, where L is the length of the rectangular graphene. These wrinkling parameters are captured through processing the atomic coordinate information calculated by LAMMPS MD codes, as shown in Fig. 3.

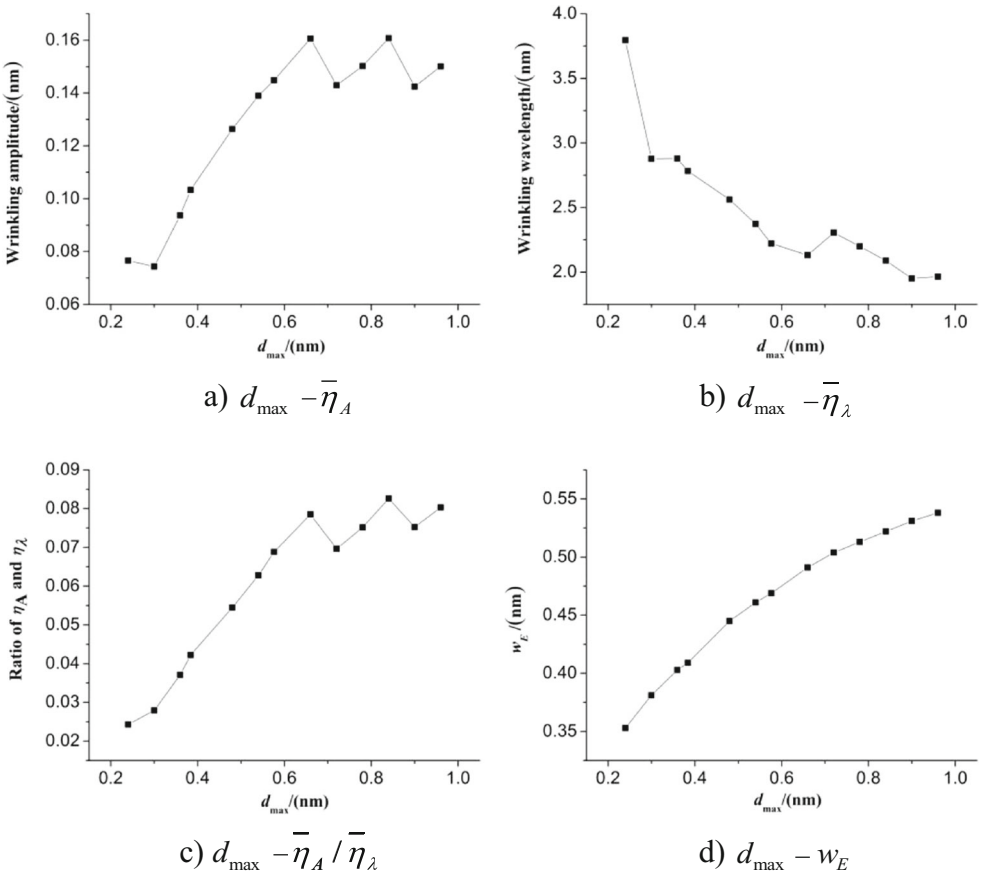

Fig. 6 Curves of wrinkling parameters over d_{max} **a** $d_{max}-\overline{\eta}_A$ **b** $d_{max}-\overline{\eta}_\lambda$ **c** $d_{max}-\overline{\eta}_A/\overline{\eta}_\lambda$ **d** $d_{max}-w_E$

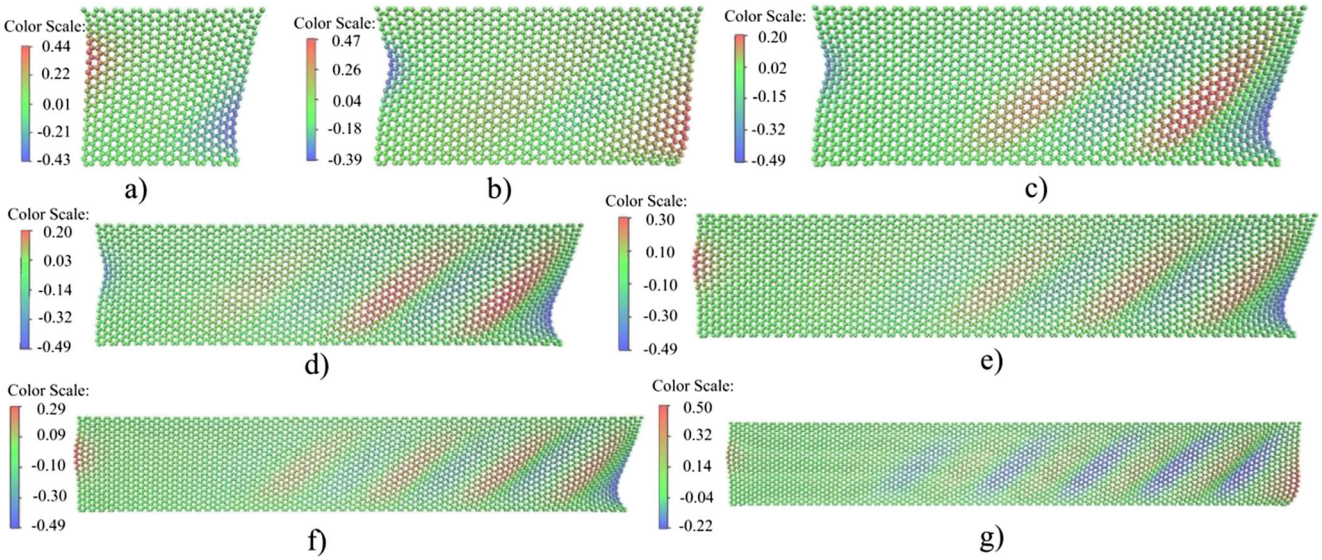

Fig. 7 Wrinkling configurations of different aspect ratio: **a**–**g** for ratio 1 to 7 for, unit: nm

Result and discussion

Wrinkling evolution

The wrinkling configurations at d_{max}=0.24, 0.48, 0.72, 0.96 nm are shown in Fig. 4. Wrinkles are formed on the SLGS surface. The morphologies and angles of these wrinkles change gradually from right to left. The wrinkles are initially generated from the right area of graphene. As d_{max} rises, the wrinkles become slender and slant toward the loading direction with the wrinkling number increasing. Wrinkling on the right region of graphene develops fast, while the one on the left grows relatively slowly. These phenomena are related to the structural shape, load and constrain condition of graphene. Led by the interaction between gradient shear and constrain condition, the wrinkling rudiment produced by the out-of-plane movement of the right free edge grows into a series of gradient changing winkling on rectangular graphene.

Table 2 Wrinkling parameters of different aspect ratios (d_{max}=0.64 nm)

Aspect ratio	$\overline{\eta}_A$ (nm)	$\overline{\eta}_\lambda$ (nm)	$\overline{\eta_A/\eta_\lambda}$	n	$n\overline{\eta}_\lambda/L$	w_E (nm)
1	0.03	1.29	0.023	1(1, 0)	0.323	0.44
2	0.12	2.27	0.055	2(1, 1)	0.568	0.47
3	0.16	2.17	0.076	3(2, 1)	0.543	0.49
4	0.15	2.28	0.073	5(3, 2)	0.713	0.49
5	0.16	2.37	0.075	7(4, 3)	0.830	0.49
6	0.17	2.23	0.082	8(4, 4)	0.743	0.49
7	0.17	2.37	0.081	10(5, 5)	0.846	0.50

Graphene surface is initially stable at first, while the free edges flow due to the relaxation process. With the d_{max} increases, the graphene structure becomes unstable and starts to wrinkle. When d_{max}=0.24 nm, two wrinkles have been produced on the graphene surface as shown in Fig. 4a), and the wrinkling number is 2(1, 1). As the d_{max} reaches 0.48 nm, a wrinkling crest has been formed in the central region of graphene, increasing the wrinkling number to 3(2, 1). Wrinkling angle increases obviously and wrinkling amplitude rises. Graphene wrinkles heavily on the right region, but slightly on the left region. When d_{max} approaches to 0.72 nm, a new wrinkling trough occurs on the left side of wrinkles and wrinkling number changes to 4(2, 2), which pushes the

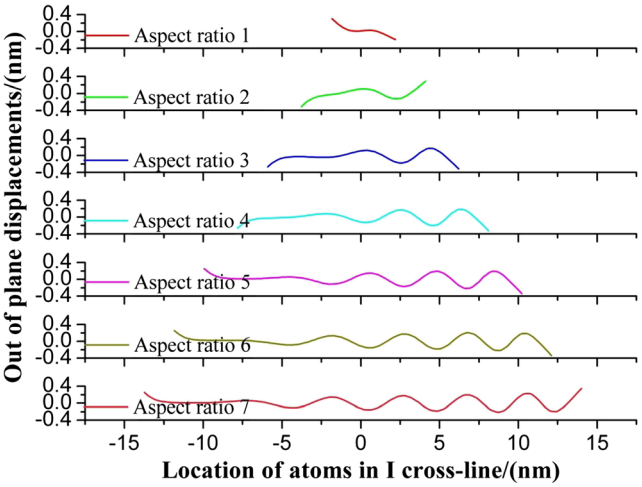

Fig. 8 Wrinkling shapes of line I of different aspect ratios

Table 3 Wrinkling parameters at different temperatures (d_{max}=0.64 nm)

Temperature	$\overline{\eta}_A$ (nm)	$\overline{\eta}_\lambda$ (nm)	$\overline{\eta_A/\eta_\lambda}$	n	$n\overline{\eta}_\lambda/L$	w_E (nm)
0.01 K	0.16	2.17	0.076	3(2, 1)	0.543	0.49
100 K	0.16	2.26	0.075	3(1, 2)	0.565	0.45
200 K	0.15	2.47	0.066	4(2, 2)	0.823	0.48
300 K	0.15	2.65	0.066	4(2, 2)	0.883	0.47
400 K	0.16	2.53	0.071	4(2, 2)	0.843	0.41
500 K	0.17	2.45	0.072	4(2, 2)	0.817	0.55

wrinkle to the right. As d_{max} gradually increases to 0.96 nm, wrinkles become slender. The wrinkling number increases to 5(3, 2) with the occurrence of the new wrinkling crest on the left region of graphene, which makes the wrinkles more crowded. The C-C bonds on the top of the right edge are stretched heavily and nearly to breaking, corresponding to the length of C-C bonds that mostly increase to 0.17 nm.

The out-of-plane displacements of the key points and wrinkles propagation direction are shown in Fig. 5. The wrinkling evolution process could be divided into three stages based on the Fig. 5, i.e., I. latency stage, II. developmental stage, and III. mature stage. After the shear displacement loads, the ripples caused by the relaxation process flow on the graphene surface, while the graphene does not wrinkle until d_{max}=0.065 nm. This stage is latency stage, occurring in 0 nm<d_{max}≤0.065 nm. After the d_{max} reaches 0.065 nm, the wrinkling evolution goes into developmental stage and terminates by d_{max}=0.974 nm. During this stage, the wrinkles are formed and develop unstably with the out-of-plane reciprocating motion of atoms. The wrinkling moves across the graphene, according to the key points' displacements developments. As the load goes on, new wrinkles are generated from the left free edge and drove the wrinkles propagating to the right. When d_{max} increases to 0.974 nm, the wrinkling development enters a steady phase and release energy, which results in the temporary increment of system temperature as shown in Fig. 2. In the meantime, the wrinkling evolution is transformed from developmental stage into the last stage mature stage, which happens in 0.974 nm<d_{max}≤1.022 nm. In this stage, wrinkling grows stably till the graphene breaks, corresponding to tempestuously variations of the key points' displacements.

The wrinkling parameters results of cross-section line I are listed in Table 1. The wrinkling amplitude $\overline{\eta}_A$, wrinkling angle $\overline{\eta}_\alpha$ and the ratio $\overline{\eta_A/\eta_\lambda}$ increases while the wrinkling wavelength $\overline{\eta}_\lambda$ decreases with the rising d_{max}, which reflects the heavily trend of graphene wrinkling. As the d_{max} increases, the wrinkling number rises from 2 to 5, while the amplitude and wavelength keep developing. The maximum of out-of-plane displacements w_E is increasing till the eve fracture of graphene, corresponding to w_E=0.54 nm. The generation and propagation of new wrinkles have an influence on the wrinkling direction, resulting in the increase of $\overline{\eta}_\alpha$. The curves of wrinkling parameters are shown in Fig. 6. There are three turning points on the curve due to the generation of new wrinkles, which affects the mean value of wrinkling parameters. In general, the $\overline{\eta}_A$, $\overline{\eta_A/\eta_\lambda}$ and w_E keep an increasing trend over d_{max}, but the wrinkling wavelength is $\overline{\eta}_\lambda$. The increasing rate of w_E slows down at larger d_{max}, while the $\overline{\eta}_\lambda$ reduces rapidly at first but slowly later. It is observed that $\overline{\eta}_\lambda$ may suddenly have a small increment owing to the formation of new wrinkles, after which $\overline{\eta}_\lambda$ continues to decrease.

Size effects

The wrinkling configuration and parameters of different aspect ratios under the same d_{max}=0.64 nm are compared. The wrinkling configurations are shown in Fig. 7, wrinkling parameters and shapes of cross-section line I are listed in Table 2 and Fig. 8. It is observed that wrinkling parameters of aspect ratio 3 stand out from the results in Table 2. That is because the wrinkling evolution of aspect ratio 3 lies in developmental stage when d_{max}=0.64 nm, and the wrinkling number development is in the transition period from 3 to 4. Meanwhile, the wrinkling progresses to the highest level of 3-wrinkles period, resulting in the outstanding wrinkling parameters. However generally, wrinkling amplitude, wrinkling wavelength, $\overline{\eta_A/\eta_\lambda}$, w_E, $n\overline{\eta}_\lambda/L$, and wrinkling number rise as the aspect ratio increases, except aspect ratio 3. It reveals that the rising aspect ratio leads to

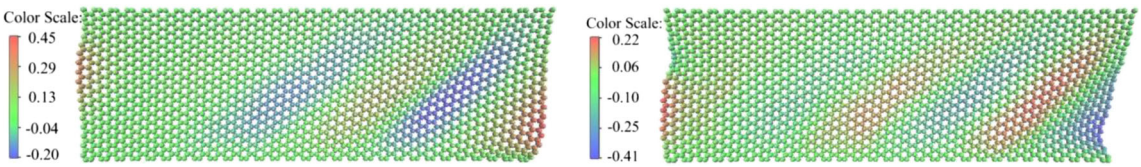

a) 100K b) 400K

Fig. 9 Wrinkling configurations at different temperatures (unit: nm) **a** 100 K **b** 400 K

Table 4 Wrinkling parameters under different loading grads (d_{max}= 0.64 nm)

k_d	$\overline{\eta}_A$ (nm)	$\overline{\eta}_\lambda$ (nm)	$\overline{\eta_A/\eta_\lambda}$	n	$n\overline{\eta}_\lambda/L$	w_E (nm)
5.000×10^{-4}	0.16	2.11	0.077	3(2, 1)	0.528	0.48
6.667×10^{-4}	0.16	2.17	0.076	3(2, 1)	0.543	0.49
8.333×10^{-4}	0.16	2.17	0.076	3(2, 1)	0.543	0.49
1.000×10^{-3}	0.16	2.14	0.077	3(2, 1)	0.535	0.49
1.167×10^{-3}	0.16	2.09	0.077	3(2, 1)	0.523	0.48
1.333×10^{-3}	0.16	2.16	0.076	3(2, 1)	0.540	0.49

more graphene wrinkles, which have a towering morphology and larger extent. The wrinkling configuration changes with the increase of the wrinkling number as the aspect ratio rises as shown in Fig. 7, reflecting the dependence of wrinkling configuration on the aspect ratio. Based on Fig. 8, it may be regarded that the wrinkling configuration extends along with the loading direction as the aspect ratio increases.

Temperature effects

The wrinkling parameters and configuration of graphene under the same d_{max}=0.64 nm and different temperature ranging from 0.01 to 500 K are shown in Table 3 and Fig. 9.

Based on Table 3, the wrinkling number rises from 3 to 4 as the temperature increases. Both the wrinkling amplitude and $\overline{\eta_A/\eta_\lambda}$ initially decreases but rises after 300 K, while the wrinkling wavelength and $n\overline{\eta}_\lambda/L$ increase initially and reduces later. There is no certain regularity between w_E and temperature. The thermal vibration of the atom is aggravated by the existence of temperature, which has a significant effect on the graphene wrinkling behavior. Wrinkling configurations at different temperatures are distinguishing as shown in Fig. 9. Wrinkling configuration at a non-zero temperature is the result of the interaction of gradient shear loading and thermal effect of graphene, indicating the great influence of temperature on graphene wrinkling deformation.

Loading grads effects

The wrinkling parameters and configurations of rectangular graphene subjected to different loading grads k_d(5.000×10^{-4} to 1.333×10^{-3}) are shown in Table 4 and Fig. 10. The differences of wrinkling parameters and configurations under the same d_{max}=0.64 nm are compared. Based on the results, the same amount of wrinkles is produced in all cases. The loading grads have an impact on the wrinkling wavelength and $n\overline{\eta}_\lambda/L$, but little on wrinkling amplitude and $\overline{\eta_A/\eta_\lambda}$. There are few discrepancies between wrinkling configurations under different k_d, as well as the w_E. Loading grads has less effect on the wrinkling deformation of graphene subjected to gradient shear.

Conclusions

The wrinkling of rectangular SLGS under gradient shear is investigated through MD simulations in this paper. The results show that wrinkles which gradually change from right to left are formed on the graphene surface. These wrinkles become crowded and slender as the loading continues. The new wrinkles are generated from the left edge driving the wrinkles to propagate to the right. These phenomena are relevant to the graphene shape and load condition. The wrinkling evolution process is divided into three stages, I. latency stage, II. developmental stage, and III. mature stage. Generally the wrinkling amplitude, maximum of out-of-plane displacements and ratio of amplitude to wavelength have an increase as the gradient-shear displacement rises, while the wrinkling wavelength decreases.

Both aspect ratio and temperature have a significant effect on wrinkling deformation of graphene subjected to gradient shear. Wrinkling configuration extends along with the loading direction with the rising aspect ratio. Wrinkling deformation of graphene at non-zero temperature is the consequence of the interaction between gradient shear and thermal effect of graphene. While the results show that the loading grads have little influence on graphene wrinkling.

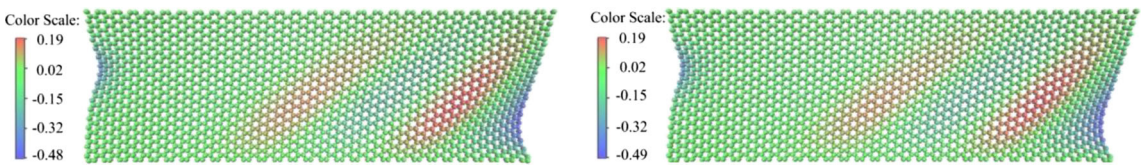

a) 5.000×10^{-4} b) 1.333×10^{-3}

Fig. 10 Wrinkling configurations under different loading grads (unit: nm) **a** 5.000×10^{-4} **b** 1.333×10^{-3}

Acknowledgments The authors wish to acknowledge the support from the National Natural Science Foundation of China (11272123, 11472108).

References

1. Bunch JS, van der Zande AM, Verbridge SS, Frank IW, Tanenbaum DM, Parpia JM, Craighead HG, McEuen PL (2007) Electromechanical resonators from graphene sheets. Science 315(5811):490–493. doi:10.1126/science.1136836
2. Meyer JC, Geim AK, Katsnelson MI, Novoselov KS, Booth TJ, Roth S (2007) The structure of suspended graphene sheets. Nature 446(7131):60–63. doi:10.1038/nature05545
3. Bao W, Miao F, Chen Z, Zhang H, Jang W, Dames C, Lau CN (2009) Controlled ripple texturing of suspended graphene and ultrathin graphite membranes. Nat Nanotechnol 4(9):562–566. doi:10.1038/nnano.2009.191
4. Wang Z, Devel M (2011) Periodic ripples in suspended graphene. Phys Rev B 83(12). doi:10.1103/PhysRevB.83.125422
5. Shen X, Lin X, Yousefi N, Jia J, Kim J-K (2014) Wrinkling in graphene sheets and graphene oxide papers. Carbon 66:84–92. doi:10.1016/j.carbon.2013.08.046
6. Pereira VM, Castro Neto AH, Liang HY, Mahadevan L (2010) Geometry, mechanics, and electronics of singular structures and wrinkles in graphene. Phys Rev Lett 105(15). doi:10.1103/PhysRevLett.105.156603
7. Ye Z, Tang C, Dong Y, Martini A (2012) Role of wrinkle height in friction variation with number of graphene layers. J Appl Phys 112(11):116102. doi:10.1063/1.4768909
8. Zhu W, Low T, Perebeinos V, Bol AA, Zhu Y, Yan H, Tersoff J, Avouris P (2012) Structure and electronic transport in graphene wrinkles. Nano Lett 12(7):3431–3436. doi:10.1021/nl300563h
9. Chen S, Li Q, Zhang Q, Qu Y, Ji H, Ruoff RS, Cai W (2012) Thermal conductivity measurements of suspended graphene with and without wrinkles by micro-Raman mapping. Nanotechnology 23(36):365701. doi:10.1088/0957-4484/23/36/365701
10. Zheng Q, Ip WH, Lin X, Yousefi N, Yeung KK, Li Z, Kim J-K (2011) Transparent conductive films consisting of ultralarge graphene sheets produced by langmuir–blodgett assembly. ACS Nano 5(7):6039–6051. doi:10.1021/nn2018683
11. Koenig SP, Boddeti NG, Dunn ML, Bunch JS (2011) Ultrastrong adhesion of graphene membranes. Nat Nanotechnol 6(9):543–546. doi:10.1038/NNANO.2011.123
12. Rafiee MA, Rafiee J, Wang Z, Song H, Yu Z-Z, Koratkar N (2009) Enhanced mechanical properties of nanocomposites at low graphene content. ACS Nano 3(12):3884–3890. doi:10.1021/nn9010472
13. Levy N, Burke SA, Meaker KL, Panlasigui M, Zettl A, Guinea F, Neto AHC, Crommie MF (2010) Strain-induced pseudo–magnetic fields greater than 300 tesla in graphene nanobubbles. Science 329(5991):544–547. doi:10.1126/science.1191700
14. Wang C, Mylvaganam K, Zhang L (2009) Wrinkling of monolayer graphene: a study by molecular dynamics and continuum plate theory. Phys Rev B 80(15). doi:10.1103/PhysRevB.80.155445
15. Gil AJ, Adhikari S, Scarpa F, Bonet J (2010) The formation of wrinkles in single-layer graphene sheets under nanoindentation. J Phys Condens Matter Inst Phys J 22(14):145302. doi:10.1088/0953-8984/22/14/145302
16. Zhang Z, Duan WH, Wang CM (2012) Tunable wrinkling pattern in annular graphene under circular shearing at inner edge. Nanoscale 4(16):5077–5081. doi:10.1039/c2nr31059g
17. Duan WH, Gong K, Wang Q (2011) Controlling the formation of wrinkles in a single layer graphene sheet subjected to in-plane shear. Carbon 49(9):3107–3112. doi:10.1016/j.carbon.2011.03.033
18. Min K, Aluru NR (2011) Mechanical properties of graphene under shear deformation. Appl Phys Lett 98(1):013113. doi:10.1063/1.3534787
19. Wang C, Liu Y, Lan L, Tan H (2013) Graphene wrinkling: formation, evolution and collapse. Nanoscale 5(10):4454–4461. doi:10.1039/c3nr00462g
20. Brenner DW, Shenderova OA, Harrison JA, Stuart SJ, Ni B, Sinnott SB (2002) A second-generation reactive empirical bond order (REBO) potential energy expression for hydrocarbons. J Phys Condens Matter 14(4):783